Science of the Total Environment 494–495 (2014) 65–73

Contents lists available at ScienceDirect

Science of the Total Environment

journal homepage: www.elsevier.com/locate/scitotenv

Incorporation of inorganic mercury (Hg^{2+}) in pelagic food webs of ultraoligotrophic and oligotrophic lakes: The role of different plankton size fractions and species assemblages

Carolina Soto Cárdenas [a,*], Maria C. Diéguez [a], Sergio Ribeiro Guevara [b], Mark Marvin-DiPasquale [c], Claudia P. Queimaliños [a]

[a] Laboratorio de Fotobiología, Instituto de Investigaciones en Biodiversidad y Medioambiente (INIBIOMA, UNComahue-CONICET), Quintral 1250, 8400 San Carlos de Bariloche, Río Negro, Argentina
[b] Laboratorio de Análisis por Activación Neutrónica, CAB, CNEA, Av. Bustillo Km 9.5, 8400, San Carlos de Bariloche, Río Negro, Argentina
[c] United States Geological Survey, 345 Middlefield Rd./MS 480, Menlo Park, CA 94025, USA

HIGHLIGHTS

- Hg^{2+} incorporation in lake plankton fractions was studied using the isotope $^{197}Hg^{2+}$.
- Hg^{2+} incorporation was assessed using three different bioconcentration factors.
- Bioconcentration factors related with fraction cell abundance, surface and biovolume.
- Picoplankton and nanoplankton lead the incorporation of Hg^{2+} in pelagic food webs.
- Mixotrophic species appear to enhance Hg incorporation via bacteria feeding.

ARTICLE INFO

Article history:
Received 8 May 2014
Received in revised form 20 June 2014
Accepted 29 June 2014
Available online xxxx

Editor: Daniel A. Wunderlin

Keywords:
Plankton
Size fractions
Hg^{2+} adsorption
Hg^{2+} internalization

ABSTRACT

In lake food webs, pelagic basal organisms such as bacteria and phytoplankton incorporate mercury (Hg^{2+}) from the dissolved phase and pass the adsorbed and internalized Hg to higher trophic levels. This experimental investigation addresses the incorporation of dissolved Hg^{2+} by four plankton fractions (picoplankton: 0.2–2.7 μm; pico + nanoplankton: 0.2–20 μm; microplankton: 20–50 μm; and mesoplankton: 50–200 μm) obtained from four Andean Patagonian lakes, using the radioisotope $^{197}Hg^{2+}$. Species composition and abundance were determined in each plankton fraction. In addition, morphometric parameters such as surface and biovolume were calculated using standard geometric models. The incorporation of Hg^{2+} in each plankton fraction was analyzed through three concentration factors: BCF (bioconcentration factor) as a function of cell or individual abundance, SCF (surface concentration factor) and VCF (volume concentration factor) as functions of individual exposed surface and biovolume, respectively. Overall, this investigation showed that through adsorption and internalization, pico + nanoplankton play a central role leading the incorporation of Hg^{2+} in pelagic food webs of Andean lakes. Larger planktonic organisms included in the micro- and mesoplankton fractions incorporate Hg^{2+} by surface adsorption, although at a lesser extent. Mixotrophic bacterivorous organisms dominate the different plankton fractions of the lakes connecting trophic levels through microbial loops (e.g., bacteria–nanoflagellates–crustaceans; bacteria–ciliates–crustaceans; endosymbiotic algae–ciliates). These bacterivorous organisms, which incorporate Hg from the dissolved phase and through their prey, appear to explain the high incorporation of Hg^{2+} observed in all the plankton fractions.

1. Introduction

In aquatic systems, mercury (Hg) is a widespread toxic element which may be present in various chemical forms, including elemental (Hg^0), inorganic (Hg^+ and Hg^{2+}) and organic forms like the neurotoxin methylmercury (MeHg) (Ullrich et al., 2001; Ravichandran, 2004). During the last decades, and due to its high degree of toxicity, an extensive body of literature has focused on the formation and biomagnification of MeHg through the aquatic food webs (Mason et al., 2000; Ullrich et al., 2001; Benoit et al., 2003; Wang et al., 2004; among others). However, among mercury forms, inorganic mercury (Hg^{2+}) is the most common chemical species in aquatic environments (Ravichandran, 2004; Wu and Wang, 2014), partially contributing through trophic transfer to

* Corresponding author.
E-mail address: sotocardenascaro@gmail.com (C. Soto Cárdenas).

http://dx.doi.org/10.1016/j.scitotenv.2014.06.138
0048-9697/

the mercury pool present at higher levels of the food web. In both marine and freshwater ecosystems, the incorporation of Hg^{2+} at the base of the pelagic food web can be highly efficient (Pickhardt et al., 2005; Stewart et al., 2008; Carroll et al., 2011). Basal organisms comprising bacteria and phytoplankton may accumulate up to 10^5 times more Hg from the aqueous phase than the organisms at higher trophic levels (Pickhardt and Fisher, 2007). Then, understanding the incorporation of Hg^{2+} at the base of the pelagic food web is essential to better delineate the pathway of Hg in the water column (Pickhardt et al., 2005; Carroll et al., 2011; Le Faucheur et al., 2014).

Despite the different magnitudes of Hg^{2+} incorporation at different levels of the food web, the partitioning of Hg is governed by a variety of environmental factors. Water chemistry parameters such as pH, and the quantity and quality of dissolved organic matter (DOM) affect the membrane's functional groups in living cells, thereby influencing their permeability and affinity for binding Hg (Mason et al., 1996; Pickhardt and Fisher, 2007). In addition, the transference of trace metals within the pelagic food web depends on several characteristics of the pelagic communities: the relative abundance of different organisms (Chen and Folt, 2005; Luengen and Flegal, 2009), their size (Fisher et al., 1983; Mason et al., 1996), and their particular surfaces (Fisher et al., 1983). The increase of individual abundance is associated with a lower degree of trace metal partitioning (Chen and Folt, 2005; Luengen and Flegal, 2009). This dilution phenomenon has been reported for rapidly growing algal blooms, which resulted in lower Hg concentrations in both algae and higher trophic level plankton (Sunda and Huntsman, 1998; Chen and Folt, 2005; Pickhardt et al., 2005; Karimi et al., 2007; Pickhardt and Fisher, 2007).

Organism size can also influence Hg uptake efficiency, with smaller organisms accumulating trace metals more rapidly than larger organisms, due to the greater surface area to volume ratio (S:V) of the former (Fisher et al., 1983). The picoplankton fraction (0.2–2 μm), comprised largely of heterotrophic bacteria and autotrophic picocyanobacteria, can rapidly assimilate trace metals given their high surface area to volume ratios and high growth rates (Fisher, 1986; Twiss and Campbell, 1995). Further, biological surfaces like mucilage, cell walls and membranes, may play an important role on the partitioning of Hg since they have functional groups with differential affinities for metals (Rajamani et al., 2007).

The incorporation of Hg into basal organisms may also be influenced by the mode of nutrition of the specific organisms. In particular, mixotrophic species can ubiquitously alternate between the autotrophic and heterotrophic nutrition. These planktonic organisms incorporate Hg passively from the surrounding environment (dissolved phase), whereas through the consumption of bacteria, they actively incorporate Hg transferring this metal to higher pelagic trophic levels and regenerating a fraction to the environment (Twiss and Campbell, 1995). Metals incorporated by these basal organisms are passed into a microbial loop, an important trophic link that includes microplanktonic consumers (<200 μm) such as heterotrophic and mixotrophic flagellates, ciliates, rotifers, and small cladocerans (Azam et al., 1983; Mitra et al., 2014). Herbivorous grazers (e.g. copepods) differentially assimilate metals contained within the cytoplasm of prey cells while egesting metals bound to cell walls and membranes (Twining and Fisher, 2004), thus having a particular assimilation efficiency for metals adsorbed to and internalized into their food particles (Reinfelder and Fisher, 1991).

Different indexes have been created to characterize the metal enrichment by planktonic organisms relative to the surrounding environment (Fisher et al., 1983). The bioconcentration factor (BCF) has been used to describe the extent to which a metal is concentrated by an organism from the surrounding environment (Gorski et al., 2008). The surface concentration factor (SCF) describes phytoplankton trace metal accumulation normalized to cell surface area, considering that passive surface adsorption is the prevailing process for Hg^{2+} incorporation (Fisher et al., 1983). The volume concentration factor (VCF) describes phytoplankton trace metal accumulation normalized to cell volume (Fisher et al., 1983; Pickhardt and Fisher, 2007; Gorski et al., 2008; Luengen et al., 2012), and is appropriate for assessing metal internalization into cells. The VCF is similar to the BCF since both express the cellular concentration including adsorbed and absorbed forms, and are both relative to the metal concentration in the aqueous phase (Luoma and Rainbow, 2008).

Nahuel Huapi National Park, located in the North Andean region of Patagonia (Argentina), is a natural, well-protected reserve. The Park limits at the west with an active volcanic region in the Andes which is considered to have a high eruptive frequency (last eruptions in 1960 and 2011) that impacts the Argentinean Patagonia due to predominant westerly winds. While mining and anthropogenic activities can be ruled out within the Park, it has been suggested that volcanic activity in the area may contribute with materials through atmospheric transport and deposition (Bubach et al., 2012; Rizzo et al., 2014). Although the particular Hg contribution through volcanic activity to the area has not been sufficiently studied as yet, there is evidence of gaseous elemental mercury (Hg^0) emissions (Higueras et al., 2013). This is in agreement with previous reports of high mercury atmospheric fluxes from volcanic activity (29 ton y^{-1}) including localities in Central and South America (Nriagu and Becker, 2003).

This North Patagonian region comprises a large number of lakes including large and deep lakes (>5 km^2, Z_{max} > 100 m) and small and shallow ones (<5 km^2, Z_{max} < 12 m) (Quirós and Drago, 1999). In Andean lakes, high levels of total mercury have been detected in pelagic compartments; up to 260 μg g^{-1} DW in phytoplankton and up to 42 μg g^{-1} DW in zooplankton (Arribére et al., 2010a; Ribeiro Guevara et al., 2010). Recent measurements of natural water samples showed that 97% of the total dissolved Hg pool was inorganic Hg^{2+} and just 3% was MeHg. Also, MeHg was reported as lower than 0.7% DW in the plankton fractions from 10 to 200 μm (Arcagni et al., 2013). The oligotrophic condition of these glacially originated lakes provides a unique opportunity to study the incorporation of Hg into complex and distinct pelagic food webs dominated by small planktonic organisms, connected through a microbial food web (Queimaliños, 2002; Bastidas Navarro et al., 2009; Gerea, 2013). In these systems, pelagic organisms compensate nutrient limitation through mixotrophy, an important trophic link between the microbial loop and the metazoan food web that may influence deeply the fate of Hg in the water column. Consequently, there is a need to better understand the relationships among natural plankton fractions, including the microbial components, as they may control the incorporation and partition of Hg into upper-trophic pelagic levels.

In this investigation we aimed to analyze the bioconcentration of Hg^{2+} into different natural plankton size fractions from one deep ultraoligotrophic lake and three shallow oligotrophic Andean Patagonian lakes, using the radioisotope $^{197}Hg^{2+}$. Our central hypothesis is that the potential for Hg^{2+} bioconcentration depends on the particular traits of each size fraction, such as the abundance and the S:V ratio. For this purpose, we measured the incorporation of $^{197}Hg^{2+}$ by plankton including organisms from 0.2 to 200 μm, fractionated by size resulting in the separation of the assemblages picoplankton, pico + nanoplankton, microplankton and mesoplankton, which differ in their ecological roles. In order to understand the process of $^{197}Hg^{2+}$ incorporation in each of these planktonic fractions, the indexes BCF, SCF and VCF were applied. This approach included the estimation of individual surface area and biovolume, calculated using the specific linear dimensions of the different organisms and the appropriate geometric models. Based on the experimental results we discuss the role of the microbial loop and the incidence of mixotrophy in relation to the Hg^{2+} bioconcentration.

We predict that small plankton size fractions will have the greatest VCF due to their higher S:V ratios, independently of their particular species composition. Regarding the BCF, we predict that the small plankton fractions will have low Hg bioconcentration values due to biodilution. Finally, we anticipate that the SCF values will depend on the different organisms' surfaces present in each fraction of the different plankton assemblages.

2. Materials and methods

2.1. Sampling sites

The natural water and plankton samples used in this study were collected from four neighboring Andean lakes; the deep ultraoligotrophic lake Moreno and the oligotrophic shallow lakes El Trébol, Morenito and Escondido (Nahuel Huapi National Park, Patagonia, Argentina). The lakes belong to the Nahuel Huapi lake catchment and they are located within an area of 12 km^2 with a maximum linear distance between sampling sites of ~6 km (Fig. 1a and b). These systems have been extensively studied and are the focus of continuous monitoring since they are representative of deep and shallow Andean lakes and, due to the fact that they are within a natural reserve. They present some differences in their limnological features as detailed in Diéguez et al. (2013), and also they have distinctive planktonic assemblages, varying fundamentally in the species composition of the 50–200 μm fraction. The mixotrophic algae *Dinobryon divergens* and *Dinobryon sertularia* may dominate that fraction together with some large diatom species (Queimaliños, 2002; Gerea, 2013). However, large mixotrophic ciliates (*Stentor araucanus* and *Ophrydium naumanni*) are conspicuously present only in the deep ultraoligotrophic lake Moreno (Queimaliños et al., 1999). The smaller size fractions could also differ in species composition among lakes. The microplanktonic fraction is constituted by different species of dinoflagellates and diatoms, while the nanoplankton is dominated by the mixotrophic flagellates *Chrysochromulina parva*, *Plagioselmis lacustris and Gymnodinium varians*, with different relative abundances among lakes (Queimaliños et al., 1998; Queimaliños, 2002; Gerea, 2013).

2.2. Water sampling and laboratory procedures

Water samples (~20 L) were collected at a central sampling point in each lake (October 2010, Austral spring), using a 12 L Schindler-Patalas trap. The samples were poured into acid-washed 20 L polycarbonate carboys and immediately transported to the laboratory, where they were processed within 2–3 h. Temperature, conductivity and pH were measured in situ with a YSI 85 probe. Total phosphorus (TP) and total nitrogen (TN) were determined directly on whole lake water following APHA (2005) and Bachmann and Canfield (1996), respectively. Dissolved organic carbon (DOC) concentrations were measured in pre-filtered water samples (Whatman GF/F; 0.7 μm) with a Shimadzu TOC-L high temperature analyzer measuring non-purgeable organic carbon. Chlorophyll *a* concentration was assessed by filtering a volume of the water samples from each site through a pre-burned glass fiber filter (GF/F). The material retained in the filters was extracted with ethanol 90% and the extracts were scanned in a UV–visible spectrophotometer (Hewlett–Packard 8453), according to Nusch (1980).

Initially, 9–16 L of the whole lake water was filtered through a net of 200 μm mesh to concentrate organisms <200 μm. Then, the mesoplanktonic fraction (50–200 μm) was obtained through a gentle and passive filtration of the pre-filtered water, using in this case a 50 μm mesh size hand net. During the procedure, the net was kept submerged allowing the concentration of the organisms in the small water volume contained by the net. The filtrate with the organisms <50 μm was subsequently sieved through a 20 μm mesh size, to obtain the microplanktonic fraction (20–50 μm). Then, 2–3 L of the volume previously filtered through the 20 μm mesh were passed through 0.2 μm PVDF filters (Millipore) and 2.7 μm GF/D filters (Whatman) applying low vacuum pressure (<15 kPa) to obtain the pico + nanoplanktonic fraction (0.2–20 μm) and the picoplanktonic fraction (0.2–2.7 μm), respectively.

In all cases, subsamples (corresponding to each fraction) were collected with a pipette from the concentrated volume retained either in the nets or in the filtration unit. The concentrated subsamples of the two smallest fractions were ultrasonicated twice at 35,000 Hz for 30 min in order to avoid flocculation. The fractions obtained as explained reflect the composition and relative abundances of the different organisms within each fraction; however, they do not reflect the actual abundances of the organisms in the natural environment.

The four plankton size-fractions obtained from each of the four lakes were maintained for 20 min at 15 °C, in darkness, and subsequently resuspended in filter-sterilized (0.2 μm PVDF filters) natural water from the corresponding lake at a final volume of 400–500 mL.

Two sets of experimental incubations were performed. Experiment 1 was designed to study the incorporation of dissolved radiolabeled Hg^{2+} (hereinafter $^{197}Hg^{2+}$) by the 0.2–20 μm, 20–50 μm and 50–200 μm plankton fractions from the four lakes. Experiment 2 was performed to study the incorporation of $^{197}Hg^{2+}$ by the 0.2–2.7 μm plankton fraction (autotrophic and heterotrophic bacteria and/or picoplankton) from the four lakes. This experiment was set up to compare among lakes the smallest and comparatively more homogeneous fraction. Experiments 1 and 2 were run separately; however the same protocol was applied to both trials. The experiments consisted of incubations of the plankton fractions plus the filter-sterilized lake water from each lake amended with $^{197}Hg^{2+}$ as control. Thus, Experiment 1 consisted of 48 samples: 4 treatments (3 plankton fractions plus one sterile control per lake), 4 lakes, all in triplicate (3 replicates per treatment/lake). Experiment 2 consisted of 24 samples: 2 treatments (0.2–2.7 μm plankton fraction plus one sterile control per lake), 4 lakes, all in triplicate (3 replicates per treatment/lake). Each experimental unit consisted of 100 mL of each plankton fraction in a 250 mL sterile stoppered Erlenmeyer flask. Once ready, all experimental units were amended with $^{197}Hg^{2+}$ to a final concentration ranging from 10 to 12 ng L^{-1} similar to natural levels. The high specific activity $^{197}Hg^{2+}$ used in these experiments was produced by irradiation of Hg (in 2% HNO_3 solution) enriched in the ^{196}Hg

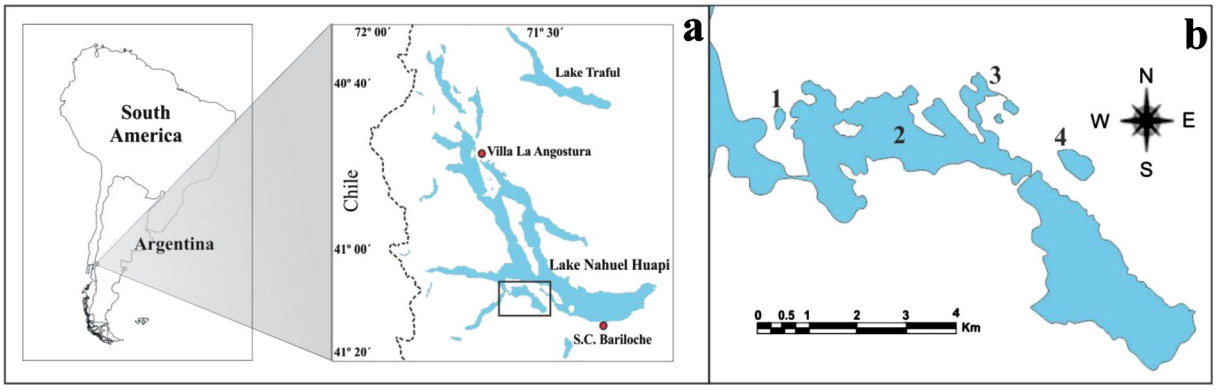

Fig. 1. a — Geographic location of the study area inside the Nahuel Huapi System (North Patagonia, Argentina); b — Map of the selected lakes for this experimental study: Lake Escondido (1), Lake Moreno West (2), Lake Morenito (3) and Lake El Trébol (4).

isotope to 51.6% (natural abundance: 0.15%) in the RA-6 nuclear research reactor ($\Phi th = 1 \times 10^{13}$ n cm^{-2} s^{-1}), Centro Atómico Bariloche, Argentina. The Hg concentration in the stock solution irradiated was 57 μg mL^{-1}; all Hg concentrations of the amendments used in the experiments were calculated relative to this value. Standards and working solutions were prepared using ASTM-1 water.

After the amendment with $^{197}Hg^{2+}$, all experimental units were incubated in an environmental chamber (Sanyo MLR5) at 15 °C in the dark for 23 h. After incubation, each experimental unit was filtered through a 0.2 μm PVDF filter. The filter-passing solution was sampled (4 mL) to determine the $^{197}Hg^{2+}$ in solution after incubation. All filters obtained were folded and placed into individual glass tubes for subsequent $^{197}Hg^{2+}$ quantification associated with the corresponding planktonic fraction. The incorporation of $^{197}Hg^{2+}$ by the various plankton fractions was obtained measuring X-ray and γ-ray emissions associated with the $^{197}Hg^{2+}$ decay, using a well type High Purity Germanium (HPGe) detector (Ribeiro Guevara et al., 2007).

2.3. Characterization of plankton fractions

Water samples (50 mL) collected from each of the treatment batches prepared just prior to the amendment of $^{197}Hg^{2+}$ were preserved for subsequent identification and quantification of the planktonic organisms. Samples of the 0.2–2.7 μm size fraction (auto and heterotrophic picoplankton) were preserved with formaldehyde–cacodylate (final concentration 10%). Subsamples for heterotrophic picoplankton (bacteria) were stained with 4′, 6-diamidino-2- phenylindole (DAPI, final concentration 0.2% w/v) (Porter and Feig, 1980). Both bacteria and autotrophic picoplankton were quantified on 0.2 μm black membrane filters (Poretics) at 1000× magnification under an epifluorescence microscope (Olympus BX50), using UV light (U-MWU filter) and blue light (U-MWB filter), respectively. Subsamples of 0.2–20 μm, 20–50 μm and 50–200 μm size fractions were preserved with 1% of acid Lugol's solution and formaldehyde solution (4%). The enumeration of the nanoplankton and microplankton fractions was performed under an inverted microscope following the Utermöhl technique (Utermöhl, 1958). The 50–200 μm plankton fraction was counted in a Sedgwick–Rafter chamber (1 mL) under direct microscope. For each plankton fraction the enumeration was performed on three replicates. The linear dimensions of at least 30 cells/individuals were measured using a graduate micrometer in order to calculate the surface and volume for each type of organism.

2.4. Data analysis

The individual surface areas (S_i, μm^2 ind^{-1}) and volumes (V_i, μm^3 ind^{-1}) of all planktonic species belonging to each size fraction were calculated using geometric models. The biovolume of picoplankton was estimated using the dimensions published by Zagarese et al. (2001), Callieri et al. (2007), Corno et al. (2009) and Gerea (2013) for the four North Patagonian lakes. Lineal dimension of phytoplankton species and ciliates was used to calculate their volume and surface according to Sun and Liu (2003), while the same morphometric parameters were calculated for rotifers and crustaceans following McCauley (1984) and Binggeli et al. (2011).

For each plankton fraction, the total exposed surface (S_t) was calculated by multiplying the surface of each specific component (S_i, μm^2 ind^1) by its abundance (ind mL^{-1}), and finally summing them up to obtain the total surface per plankton fraction (S_t, μm^2 mL^{-1}). Similarly, the total volume per fraction (V_t) was calculated multiplying the specific V_i (μm^3 ind^{-1}) by its abundance (ind mL^{-1}) and summing them up. The surface to volume ratio of each type of organism (S_i:V_i, μm^{-1}) was calculated, and the total surface to the volume ratio of each fraction (S_t:V_t) was determined as the weighted average taking into account the abundance of each taxa. The mean individual exposed surface of each fraction (S_f, μm^2 ind^{-1}) was calculated as S_t divided by the total individual abundance of the fraction. The same procedure was applied to calculate the mean volume of each fraction (V_f, μm^3 ind^{-1}).

The $^{197}Hg^{2+}$ incorporation by the different fractions was corrected for the $^{197}Hg^{2+}$ retention on the filters by subtracting the $^{197}Hg^{2+}$ quantified for the control filter (without plankton). Hg incorporation was calculated for each experimental unit based upon the initial amendment of $^{197}Hg^{2+}$ compared to the final Hg activity.

Three bioconcentration factors were calculated in relation to: i) cell or individual abundance (BCF), ii) cell or individual biovolume (VCF) and, iii) exposed surface (SCF).

The factors were calculated as follows:

$$BCF = CA/CW\left(\text{pL ind}^{-1}\right)$$
$$VCF = CB/CW\left(\text{pL } \mu\text{m}^{-3}\right)$$
$$SCF = CS/CW\left(\text{pL } \mu\text{m}^{-2}\right)$$

where:

CA	concentration of $^{197}Hg^{2+}$ measured in the organisms (ag ind^{-1})
CW	concentration of $^{197}Hg^{2+}$ measured in the aqueous medium (ag pL^{-1})
CB	concentration of $^{197}Hg^{2+}$ measured per unit of biovolume (ag μm^{-3})
CS	concentration of $^{197}Hg^{2+}$ measured per unit surface (ag μm^{-2})
pL	picoliter
ag	attogram

Plankton fraction abundance, the ratio S_t:V_t and the Hg^{2+} concentration factors (BCF, VCF and SCF) obtained, were tested for normality (Kolmogorov–Smirnoff, Normality test) and homoscedasticity before performing the two-way analysis of variance (ANOVA), to evaluate differences in Hg^{2+} incorporation among lakes and among plankton fractions within the same lake. The 0.2–2.7 μm fraction was not individually considered in the different statistical analyses since it overlaps with the fraction 0.2–20 μm, and because the experiments were run in different days. The relationships between surface and volume of each plankton fraction were fitted to simple linear models. Independent post hoc comparisons were performed to evaluate differences in the total abundance, BCF, VCF and SCF among the plankton fractions studied. Correlation analysis (Pearson product moment correlation) was performed to explore the relationships between the BCF and the total cell abundance, and between the bioconcentration factors VCF and SCF.

3. Results and discussion

3.1. Limnological features of the study lakes at the time of sample collection

The four lakes sampled for natural water and plankton presented a gradient in terms of water chemistry and other indicators. The wider range in water chemistry was represented by DOC which ranged between extremely low values in the ultraoligotrophic Lake Moreno (0.5 mg L^{-1}) followed by lakes El Trébol, Morenito and at last by Lake Escondido (3.9 mg L^{-1}) (Table 1). TP was lowest in Lake Moreno followed by lakes Escondido and Morenito with the highest concentration in Lake El Trébol. TN showed a similar trend than TP among lakes. The pH values ranged between 7.2 and 7.6 while conductivity varied between 36 and 72 μS cm^{-1}. Chlorophyll and nutrient concentrations were lowest in Lake Moreno as compared to the four other lakes (Table 1). Overall, these parameters reflect the ultraoligotrophic condition of the deep lake Lake Moreno and the oligotrophic status of the remaining shallow lakes.

Table 1
Geographic location and limnological features of the Andean–Patagonian lakes Moreno, El Trébol, Morenito and Escondido at the time of sampling collection (October 2010). References: Z_{max} = maximum depth; DOC = dissolved organic carbon; TP = total phosphorus and TN = total nitrogen concentrations; n.d = not determined.

Lake feature	L. Moreno	L. Morenito	L. El Trébol	L. Escondido
Location	41°03′S, 71°32′W	41°03′S, 71°31′W	41°04′S, 71°30′W	41°03′S, 71°34′W
Surface area (km^2)	6.1	0.4	0.3	0.1
Z_{max} (m)	90	12	12	8
Temperature (°C)	9.2	10.1	10.0	10.5
Conductivity ($\mu S\ cm^{-1}$)	42	72	36	62
pH	7.21	7.60	7.46	7.55
Dissolved O_2 ($mg\ L^{-1}$)	8.8	10.6	9.6	10.1
Chlorophyll *a* ($\mu g\ L^{-1}$)	1.1	1.0	2.4	0.8
DOC ($mg\ L^{-1}$)	0.5	3.2	2.3	3.9
TP ($\mu g\ L^{-1}$)	1.7	8.4	10.1	3.6
TN ($\mu g\ L^{-1}$)	126.3	382.4	n.d.	241.9

3.2. Plankton composition of experimental size fractions

The composition and abundance of the plankton fractions in Experiment 1 (0.2–20 μm, 20–50 μm and 50–200 μm) and in Experiment 2 (0.2–2.7 μm) revealed some similarities among lakes, but also some distinctive features (Fig. 2a and b).

In Experiment 1, the fraction 0.2–20 μm had the highest cell abundance in the four lake water treatments; whereas the fractions greater than 20 μm were several orders of magnitude lower. However, the 50–200 μm fraction had higher abundance than the 20–50 μm fraction in all lake treatments (Fig. 2a; Supplementary Table S1). The highest abundance in the fraction 50–200 μm was due to the presence of the colonial chrysophycean *Dinobryon* spp. in the experimental concentrates from lakes El Trébol, Morenito and Moreno. In terms of composition, the fraction 0.2–20 μm was found to be constituted in ~99% by picoplankton and just in ~1% by nanoplankton. The nanoplankton of the experimental filtrates was dominated by the flagellate *C. parva* in lakes Moreno, El Trébol and Escondido, whereas *P. lacustris* prevailed in the filtrates of Lake Morenito. Within the 20–50 μm fraction, *D. sertularia* and the flagellate *Cryptomonas* spp. were co-dominant in concentrates from Lake El Trébol, while the diatom *Fragilaria* spp. in combination with other less represented species, were found in the remaining lakes' experimental filtrates. The 50–200 μm fraction was dominated by *D. divergens* and *D. sertularia* in Lake Moreno and Morenito; whereas, *D. sertularia* dominated in Lake El Trébol, and *Aulacoseira granulata* in Lake Escondido. These community assemblages are consistent with previous data of these ultra-oligotrophic and oligotrophic Andean lakes (Queimaliños, 2002; Bastidas Navarro et al., 2009; Gerea, 2013).

In Experiment 2, the 0.2–2.7 μm fraction was dominated by heterotrophic bacteria followed by picocyanobacteria. This composition pattern was fairly constant in each of the four lake experimental concentrates, with heterotrophic bacteria accounting for ~95% and picocyanobacteria for the remaining 5% of the composition (data not shown). The proportions of the different planktonic groups in Experiments 1 and 2 were analyzed as percent of the total exposed surface (%S_t). The details of the contribution of the different groups of organisms in each fraction are presented in the Supporting Results (Supplementary Fig. S1).

The relationship between the mean volume (V_f) and mean exposed surface (S_f) of the different plankton fractions showed some relevant features to relate with Hg incorporation. First, within each size class and across the four lakes, the relationship between these two morphological descriptors was positive and significant ($p < 0.05$). In other words, the higher the V_f the higher the S_f within each plankton fraction. The regression slope for the relationship S_f *vs* V_f was highest for the fractions 0.2–2.7 μm and 0.2–20 μm, followed by the 20–50 μm fraction, and lastly by the 50–200 μm fraction (slope values 7.97; 3.23; 0.93 and 0.07, respectively) (Fig. 3). The differences in the slopes reflect the differences in the mean surface:volume ratios among the four size fractions, which in fact strongly define the degree of the interaction of the different fractions with the surrounding environment. In terms of Hg incorporation, the higher the surface:volume ratio of the cell/fraction the higher its Hg adsorption.

3.3. Bioconcentration of mercury by different plankton fractions

The incorporation of Hg^{2+} per cell or BCF varied significantly among lakes ($F = 197.04$, $p < 0.001$) with overall higher values in Lake Morenito, followed by Escondido, Moreno and at last by Lake El Trébol. Across lakes and within each lake a significant general trend in the BCF was found: the fraction 20–50 μm had higher BCF than the fraction

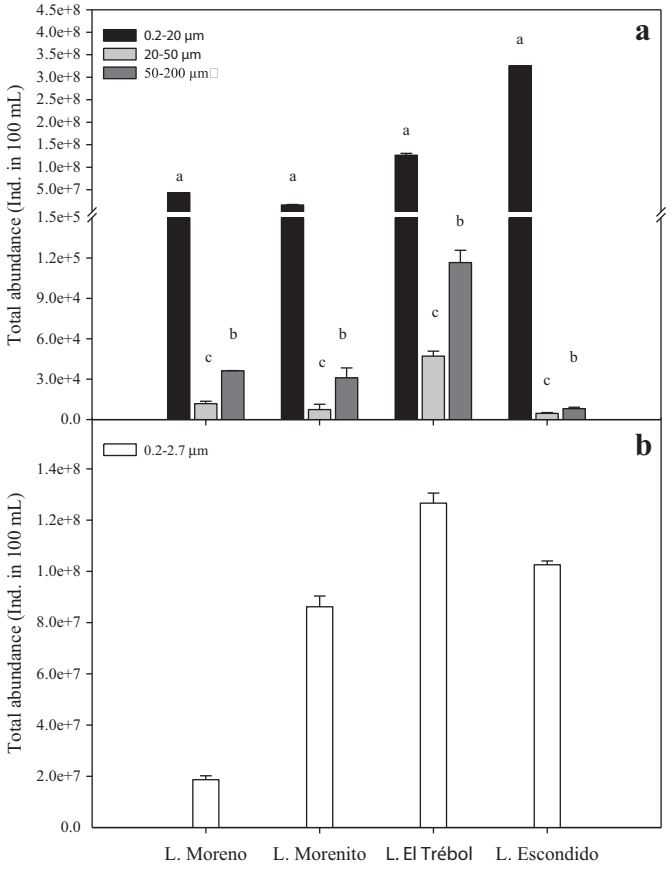

Fig. 2. a — Mean abundance of individuals per experimental unit in the different plankton fractions (0.2–20 μm, 20–50 μm and 50–200 μm) using natural water of the Andean lakes Moreno, Morenito, El Trébol and Escondido (Experiment 1). Lower case letters on top of the bars and lines indicate homogeneous groups as revealed by independent contrasts ($p < 0.05$); b — Mean abundance of individuals per experimental unit in the plankton fraction 0.2–2.7 μm in natural water of the Andean lakes Moreno, Morenito, El Trébol and Escondido (Experiment 2). Error bars represent the standard deviation of the mean.

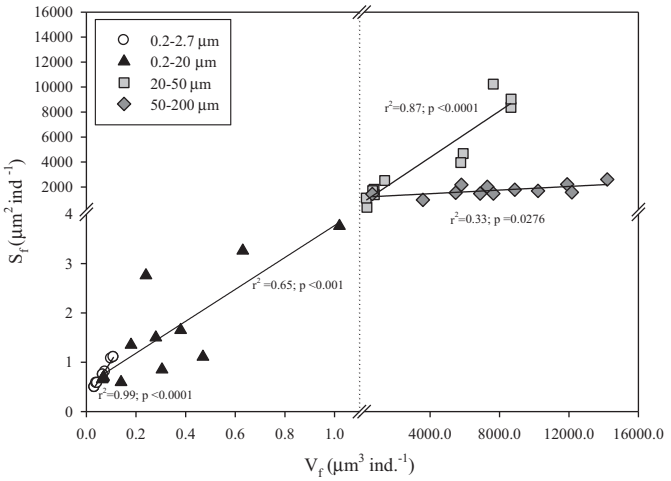

Fig. 3. Relationship between total exposed surface (S_f) and the total volume (V_f) of the plankton fractions 0.2–2.7 µm, 0.2–20 µm, 20–50 µm and 50–200 µm in the experimental treatments using natural water of the Andean lakes Moreno, Morenito, El Trébol and Escondido (Experiments 1 and 2). Lines are the simple lineal models adjusted to the S_f vs V_f for each plankton fraction.

50–200 µm, followed finally by the fraction 0.2–20 µm ($F = 1112.32$ and $F = 77.8$, $p < 0.001$, respectively) (Fig. 3a; Supplementary Table S1). This trend was confirmed by the significant negative correlations found between the BCF and total cell/individual abundance (Supplementary Fig. S2). Given the differences in the magnitude of cell/individual abundances between the fractions <20 µm and >20 µm, separate correlations were performed, resulting in similar significant patterns in both cases: the decrease of the BCF with increasing abundance of cell/organism (<20: $r = -0.92$ and >20 µm: $r = -0.86$, $p < 0.05$). In Experiment 2, the mean BCF of the fraction 0.2–2.7 µm ranged between 113 and 340 pL ind^{-1} across lakes, values within the range measured for the 0.2–20 µm fraction in Experiment 1 (Fig. 4b, Supplementary Table S1). This clearly shows the comparatively higher incorporation of $^{197}Hg^{2+}$ by the bacteria dominated fractions and, overall, the decrease in the incorporation of $^{197}Hg^{2+}$ with increasing cell abundance, a phenomenon recognized as biodilution. According to the "bloom dilution hypothesis", when phytoplankton density increases, a lower amount of metal is bound to the cells reducing their mass-specific burden (Pickhardt et al., 2002; Chen and Folt, 2005). Additionally, the "growth dilution hypothesis" considers that when growth rates of organisms exceed metal uptake rates, mass-specific Hg concentrations are lower (Sunda and Huntsman, 1998). The growth rates of picoplankton can be several times faster than in organisms that comprise the microplankton and mesoplankton. Thus, biodilution and growth dilution are both factors that may have led to the low BCF values observed in the 0.2–2.7 µm and 0.2–20 µm fractions. Furthermore, the fact that the 20–50 µm fraction had both the lowest abundance and the highest BCF values is also consistent with the idea that biodilution may limit Hg^{2+} incorporation into the smallest and more abundant plankton fractions.

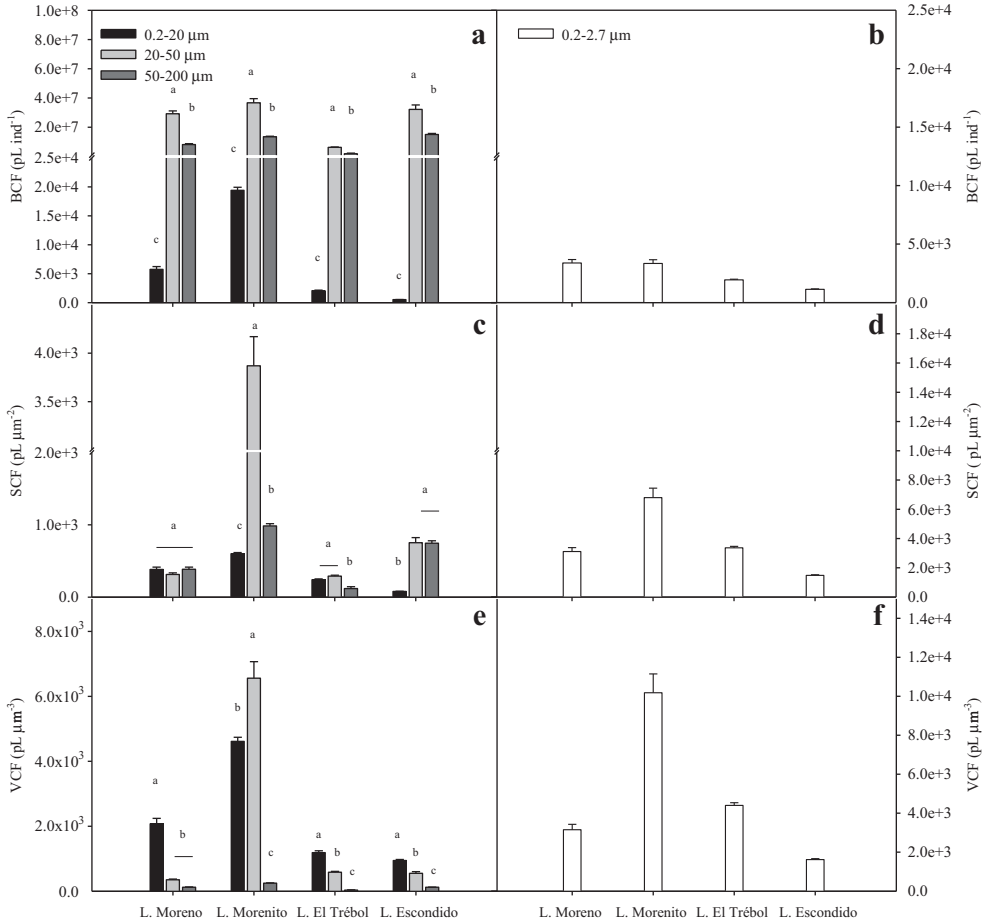

Fig. 4. Hg^{2+} concentration factors of the different plankton fractions (0.2–2.7 µm, 0.2–20 µm, 20–50 µm and 50–200 µm) in Experiments 1 and 2 using natural water of Lake Moreno, Morenito, El Trébol and Escondido: a) BCF: Hg^{2+} bioconcentration expressed in pL ind^{-1} in the plankton fractions 0.2–200 µm; b) BCF: in the plankton fraction 0.2–2.7 µm; c) SCF: Hg^{2+} bioconcentration expressed in pL µm^{-2} in the plankton fractions 0.2–20 µm, 20–50 µm and 50–200 µm; d) SCF in the plankton fraction 0.2–2.7 µm; e) VCF: Hg^{2+} volume concentration factor in the plankton fractions 0.2–20 µm, 20–50 µm and 50–200 µm, and, f) VCF in the plankton fraction 0.2–2.7 µm. Lower case letters and lines on top of the bars indicate homogeneous groups as revealed by independent contrasts ($p < 0.05$). Error bars represent the standard deviation of the mean.

Although the ambient bioavailability of Hg depends on water chemistry (e.g. DOM), the differences in planktonic Hg^{2+} incorporation observed among lakes may derive from differences in cell abundances or species composition within each lake. Planktonic surface area and cell size are major determinants controlling Hg^{2+} incorporation from the surrounding environment, since surface adsorption is a dominant mechanism by which phytoplankton accumulates trace metals in general (Fisher et al., 1983; Mason et al., 1996; Pickhardt and Fisher, 2007).

The incorporation of $^{197}Hg^{2+}$ per surface unit or SCF varied among lakes and size fractions ($F = 582.7$ and $F = 376.61$, $p < 0.001$ respectively), showing an idiosyncratic pattern among different size fractions in each lake ($F = 275.14$, $p < 0.001$) (Fig. 4c). In Lake Moreno, the SCF was similar in the three plankton fractions ($p > 0.05$). In Lake Morenito, the SCF was highest in the fraction 20–50 μm followed by the fraction 50–200 μm and by the fraction 0.2–20 μm ($p < 0.05$). In Lake Escondido the fractions 20–50 μm and 50–200 μm had similar SCFs ($p > 0.05$), which were significantly higher than that of the 0.2–20 μm fraction ($p < 0.05$). In Lake El Trébol the fractions 0.2–20 μm and 20–50 μm had similarly higher SCF values than the fraction 50–200 μm ($p < 0.05$) (Fig. 4c). In Experiment 2, the mean SCF of the fraction 0.2–2.7 μm ranged between 148 and 680 pL ind^{-1} across lakes (Fig. 4d, Supplementary Table S1). These results reflect in one hand the high contribution of the picoplankton to the pico + nanoplankton fraction and confirm the high incorporation of $^{197}Hg^{2+}$ per surface unit by bacteria.

The absence of a consistent trend in SCF values among size fractions across the four lakes examined may reflect not only the differences in community composition but also differences in parameters known to affect Hg uptake, such as water chemistry. In fact, Diéguez et al. (2013) showed differential incorporation of $^{197}Hg^{2+}$ in monospecific cultures of *Cryptomonas* in water from the same lakes, concluding that Hg uptake by algal cells decreased with the concentration of DOM. Nevertheless, in the present study the distinctive community structures found in all lakes may be a major factor accounting for the particular patterns found in the SCF. The similar and low SCF shown by the different size fractions in Lake Moreno may reflect its unique species composition and its trophic structure dominated by mixotrophic organisms (Supplementary Fig. S1). In this trophic scenario, the mixotrophic nanoflagellates included in the fraction 0.2–20 μm, feed on bacteria obtaining Hg^{2+} directly from the water and also Hg^{2+} associated with their prey. The two larger size fractions, comprising dinophyceans such as *Peridinium* spp., *Gymnodinium* spp. and mixotrophic ciliates, have the potential to scavenge Hg^{2+} from the water and also through bacteria consumption (Stoecker, 1999) and/or association (Alverca et al., 2002). However, in our experimental set-up, mixotrophy may have influenced the incorporation of Hg^{2+} into nanoflagellates, while in the two larger fractions the dissolved Hg^{2+} was likely incorporated passively since potential prey was excluded.

Some investigations have acknowledged the importance of microbial food webs in trace metal incorporation and transfer to higher trophic levels in marine, oligotrophic and ultraoligotrophic pelagic food webs (Twiss and Campbell, 1998; Twining and Fisher, 2004). Picoplanktonic organisms preyed on by macrozooplankton have an enormous potential to scavenge and assimilate dissolved traced metals owing to their high S:V ratios and rapid growth rates. The consumers in these food webs are microplanktonic species from different groups such as rotifers, dinoflagellates, ciliates and heterotrophic and mixotrophic nanoflagellates (Fisher, 1985; Twiss and Campbell, 1995).

The organisms comprising each size fraction may also have very different surface qualities which may directly influence their affinity for Hg^{2+}. Mucilage, cell walls, membranes and exoskeletons have varying functional groups with differential affinities for metals (Fisher, 1986; Rajamani et al., 2007). Moreover, the organic films covering living and non-living particles can constitute a suitable substrate for bacteria and, in fact, usually hold an associated prokaryotic biota. More recent investigations have found that Hg^{2+} accumulation is a function of binding to the ubiquitous organic film found coating all aquatic particles, living and non-living (Pickhardt and Fisher, 2007; Luengen and Flegal, 2009).

It appears that our experimental results highlight a combination of factors that ultimately regulate the incorporation of Hg^{2+}. In the complex assemblages of organisms comprised in each size fraction, different affinities for Hg^{2+} may be better approached using integrated surface, volume and abundance information.

The VCF, showed overall differences in the Hg^{2+} incorporation among lakes ($F = 862.3$, $p < 0.001$) and among plankton fractions within lakes ($F = 606.2$, $p < 0.001$). The pattern of variation of the VCF among fractions differed in some cases within each lake ($F = 263.3$, $p < 0.001$). In lakes Moreno, El Trébol and Escondido, the highest mean VCF values were associated to the 0.2–20 μm fraction, followed by the 20–50 μm fraction and then by the 50–200 μm fraction (Fig. 4e; Supplementary Table S1). In the case of Lake Morenito the 20–50 μm fraction had the highest mean VCF values, followed by the 0.2–20 μm and 50–200 μm fractions ($p < 0.05$) (Fig. 4e; Supplementary Table S1). These results suggest that the smaller size fractions are the most efficient in scavenging Hg^{2+} from the dissolved phase. Additionally, these results indicate a greater degree of internalization or Hg transfer from the surface to the cytoplasm in unicellular organisms as compared to multicellular and metazoans. The exceptionally higher VCF values of the 20–50 μm fraction measured in Lake Morenito may be due to the presence of the mixotrophic chrysophycean *Dinobryon* spp. which may experience a great deal of Hg internalization due to its high S:V. In Experiment 2, the VCF determined in the 0.2–2.7 μm fraction of the four lakes were of similar magnitude than those VCF of the fraction 0.2–20 μm found in Experiment 1 (Fig. 4f; Supplementary Table S1), reinforcing the idea that the picoplankton defines the high Hg^{2+} incorporation.

The VCF and SCF indexes were positively correlated (0.2–2.7 μm: $r = 0.99$; 0.2–20 μm: $r = 0.94$; 20–50 μm: $r = 0.99$, and 50–200 μm: $r = 0.91$; $p < 0.001$ in all cases) (Fig. 5). VCF–SCF correlations close to a 1:1 relationship (dotted line in Fig. 5) can be interpreted as that most of the Hg^{2+} is incorporated onto the surface of the different organisms. Following the same rationale, VCF–SCF correlations well above the 1:1 line would indicate a degree of Hg^{2+} internalization. The size fractions closest to the 1:1 line were the two largest ones (20–50 μm and 50–200 μm). These two larger size fractions also had comparatively lower S:V ratios, which may partially explain the lower bioconcentration observed per unit surface or volume (Supplementary Table S1). Rotifers and crustaceans are known to have a lower Hg^{2+} adsorption from the surrounding medium compared to their dietary

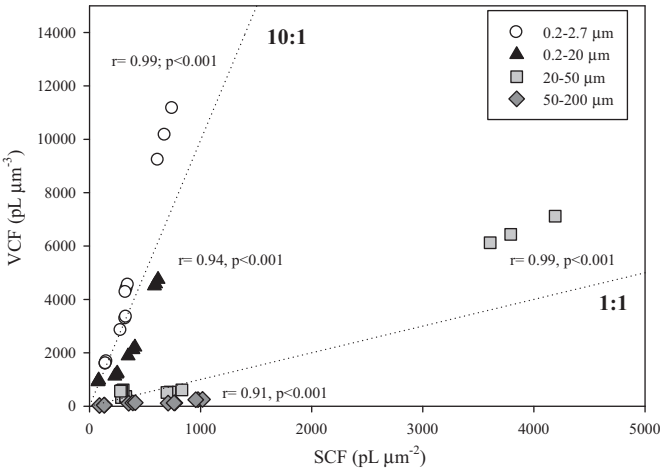

Fig. 5. Relationship between SCF (pL μm^{-2}) and VCF (pL μm^{-3}) of the four natural plankton fractions 0.2–2.7 μm, 0.2–20 μm, 20–50 μm and 50–200 μm in experimental incubations with natural water of four Andean lakes. The dotted lines refer to a 1:1 and 10:1 relationship between SCF and VCF; Pearson correlation coefficients and significance are shown close to the corresponding symbols.

uptake (Diéguez et al., 2013). In our experimental set-up, animals were starved to avoid dietary acquisition of Hg, thereby restricting Hg incorporation exclusively to Hg^{2+} in solution, which may explain their comparatively lower VCF values. The efficiency of zooplankton at assimilating ingested metals is related to the distribution of the metal within the phytoplankton cell (Reinfelder and Fisher, 1991). Planktonic grazers assimilate the metals contained within the cytoplasm of prey cells and egest metals bound to cell walls and membranes. In fact, grazers assimilate up to four times more MeHg from the phytoplankton cytoplasm than the Hg^{2+} bound to phytoplankton membranes (Mason et al., 1996). This has been implied in the explanation of the higher bioaccumulation and biomagnification of MeHg compared to Hg^{2+} (Reinfelder and Fisher, 1991; Mason et al., 1996).

The two smaller size fractions (0.2–2.7 μm and 0.2–20 μm), composed of bacteria, picocyanobacteria and nanoflagellates, showed VCF: SCF ratios closer to the 10:1 reference line (Fig. 5) indicating a much higher adsorption and also the internalization of Hg^{2+}. Previous investigations have also indicated that the picoseston size class is the most effective in scavenging Hg in mesotrophic and oligotrophic water (Twiss et al., 1996, 2003; Adams et al., 2009). This may reflect the extremely high S:V ratios (Fig. 3) and rapid growth rates characteristic of the picoplanktonic and nanoplanktonic size fractions, compared to larger pelagic organisms, as has been suggested by Fisher (1985). The cellular walls and membranes of these small organisms appear to constitute a permeable barrier for Hg^{2+} given the degree of Hg^{2+} internalization found in our experiments. Unicellular organisms have a basal role in food webs, being either heterotrophic or autotrophic and taking advantage of organic and inorganic compounds from the dissolved phase. This type of nutrition involves passive as well as active transport through the cellular wall and membrane. Moreover, organisms such as mixotrophic flagellates and ciliates can ingest algal and bacterial cells through phagocytosis, concentrating metals from their prey with internally and externally bound metals (Twining and Fisher, 2004).

The bias towards a greater abundance of small and fast reproducing organisms is directly related to a high rate of Hg regeneration in the dissolved phase. However, this regenerated Hg appears to be more recalcitrant and not as readily bioavailable (Twiss and Campbell, 1995). These authors showed that the particulate-bound metals were regenerated through grazing activity into forms less available for re-sorption by picoplankton than were the same metals in equilibrium with the inorganic ligands present in the initial medium. This observation constitutes an evidence of the direct influence of microbial organisms on the flux of Hg into higher trophic levels of the pelagic food web, previously suspected (Arribére et al., 2010b). The prevalence of mixotrophic species in the planktonic assemblages in Andean Patagonian lakes likely explain the comparatively higher total mercury content of the nanoplankton and microplankton as compared to mesoplankton in these systems.

4. Conclusions

The structure of the planktonic communities influences the incorporation and fate of Hg^{2+} in aquatic food webs. In particular, in ultraoligotrophic and oligotrophic lakes like those examined in this investigation, the partitioning of Hg^{2+} is governed by biotic factors such as the prevalence of the small organisms, the presence and relative abundance of mixotrophic species, which connect trophic levels through microbial loops (i.e. bacteria–nanoflagellates–crustaceans; bacteria–ciliates–crustaceans; and endosymbiotic algae–ciliates).

Overall, this investigation showed that through both adsorption and internalization, pico + nanoplankton play a central role in mediating the incorporation of Hg^{2+} in pelagic food webs of Andean Patagonian lakes. Larger planktonic organisms included in the micro- and mesoplankton also incorporate Hg^{2+}. Our results are consistent with the idea that mixotrophic species in the pico + nanoplankton, micro and mesoplankton fractions may enhance Hg incorporation via consumption of bacteria. The prevalence of organisms linked to the microbial food web in the pelagic zone of these lakes, may also contribute to the regeneration of Hg to the dissolved phase, as a result of the ingestion–egestion processes. The fraction of Hg not being recycled in the water column would subsequently represent a sink out of the pelagic compartment, via plankton and detritus settling to the bottom.

The choice of metrics that are used to describe the incorporation of Hg^{2+} at the base of the pelagic food web may reveal the magnitude of the different incorporation processes. Our results suggest that the BCF is a good metric to express the biodilution and/or bioconcentration of Hg, while, the SCF is better to describe the adsorption of Hg to surface. Additionally, the VCF can express the cellular concentration adsorbed and absorbed, thereby providing a measurement of the total Hg present in the organism in relation to its concentration in the surrounding environment. Hg incorporation within planktonic trophic networks may be better assessed through a combination of several metrics that quantify the size, shape and abundance of the various organisms present in a given community.

Acknowledgments

This work was funded by Consejo Nacional de Investigaciones Científicas y Técnicas (CONICET PIP 11220100100064), Agencia Nacional de Promoción Científica y Tecnológica (ANPCyT PICT 2007-393 and PICT 2012-1200) and by the International Atomic Energy Agency (IAEA), Project ARG/7/007. The authors wish to express their gratitude to Karen Riva Murray, Ph.D. Ecologist (U.S. Geological Survey) for her valuable comments on an early version of the manuscript. We are grateful to Dr. Mariana Reissig for drawing the map of the study area from satellite images. We thank the San Carlos de Bariloche Town Council and the Administration of the Nahuel Huapi National Park (APN) for granting permission to sample the lakes within their jurisdictions.

Carolina Soto Cárdenas is a CONICET Doctoral Fellow, Maria Diéguez and Claudia Queimaliños are CONICET researchers.

Appendix A. Supplementary data

Supplementary data to this article can be found online at http://dx.doi.org/10.1016/j.scitotenv.2014.06.138.

References

Adams RM, Twiss MR, Driscoll CT. Patterns of mercury accumulation among seston in lakes of the Adirondack mountains, New York. Environ Sci Technol 2009;43(13):4836–42.

Alverca E, Biegala I, Kennaway G, Lewis J, Franca S. In situ identification and localization of bacteria associated with *Gyrodinium instriatum* (Gymnodiniales, Dinophyceae) by electron and confocal microscopy. Eur J Phycol 2002;37:523–30.

APHA. Standard methods for the examination of water and wastewater. Washington DC: American Public Health Association; 2005.

Arcagni M, Campbell LM, Arribére MA, Marvin-DiPasquale M, Rizzo A, Ribeiro Guevara S. Differential mercury transfer in the aquatic food web of a double basined lake associated with selenium and habitat. Sci Total Environ 2013;454–455:170–80.

Arribére MA, Campbell LM, Rizzo AP, Arcagni M, Revenga J, Ribeiro Guevara S. Trace elements in plankton, benthic organisms, and forage fish of Lake Moreno, Northern Patagonia, Argentina. Water Air Soil Pollut 2010a;212:167–82.

Arribére M, Diéguez MC, Ribeiro Guevara S, Queimaliños CP, Fajon V, Reissig M, et al. Mercury in an ultraoligotrophic North Patagonian Andean lake (Argentina): concentration patterns in different components of the water column. J Environ Sci 2010b;22(8):1171–8.

Azam F, Fenchel T, Field J, Gray JS, Meyer-Reil LA, Thingstad F. The ecological role of water-column microbes in the sea. Mar Ecol Prog Ser 1983;10:257–63.

Bachmann RW, Canfield DE. Use of an alternative method for monitoring total nitrogen concentration in Florida lakes. Hydrobiologia 1996;323:1–8.

Bastidas Navarro M, Modenutti B, Callieri C, Bertoni R, Balseiro E. Balance between primary and bacterial production in North Patagonian shallow lakes. Aquat Sci 2009;43:867–78.

Benoit JM, Gilmour CC, Heyes A, Mason RP, Miller CL. Geochemical and biological controls over methylmercury production and degradation in aquatic ecosystems. In: Cai Y, Braids OC, editors. Biogeochemistry of environmentally important trace element, 835. American chemical society symposium series; 2003. p. 262–97.

Binggeli C, Waring A, Mihuc T. Methods for determining new biovolumes for copepods, cladocerans. Scient Discip 2011;5:25–33.

Bubach D, Pérez Catán S, Arribére MA, Ribeiro Guevara S. Bioindication of volatile elements emission by the Puyehue-Cordón Caulle (North Patagonia) volcanic event in 2011. Chemosphere 2012;88:584–90.
Callieri C, Modenutti B, Queimaliños C, Bertoni R, Balseiro E. Production and biomass of picophytoplankton and larger autotrophs in Andean ultraoligotrophic lakes: differences in light harvesting efficiency in deep layers. Aquat Ecol 2007;41:511–23.
Carroll RWH, Memmott J, Warwick JJ, Fritsen CH, Jean-Claude JB, Acharya K. Seasonal variation of mercury associated with different phytoplankton size fractions in Lahontan Reservoir, Nevada. Water Air Soil Pollut 2011;217:221–32.
Chen CY, Folt CL. High plankton densities reduce mercury biomagnification. Environ Sci Technol 2005;39(1):115–21.
Corno G, Modenutti BE, Callieri C, Balseiro EG, Bertoni R, Caravati E. Bacterial diversity and morphology in deep ultraoligotrophic Andean lakes: Role of UVR on vertical distribution. Limnol Oceanogr 2009;54(4):1098–112.
Diéguez MC, Queimaliños CP, Ribeiro Guevara S, Marvin-DiPasquale M, Soto Cárdenas C, Arribére MA. Influence of dissolved organic matter character on mercury incorporation by planktonic organisms: an experimental study using oligotrophic water from Patagonian lakes. J Environ Sci 2013;25(11):1980–91.
Fisher NS. Accumulation of metals by marine picoplankton. Mar Biol 1985;87:137–42.
Fisher NS. On the reactivity of metals for marine phytoplankton. Limnol Oceanogr 1986;31(2):443–9.
Fisher NS, Bjerregaard P, Fowler SW. Interactions of marine plankton with transuranic. 1. Biokinetics of neptunium, plutonium, and californium in phytoplankton. Limnol Oceanogr 1983;28(3):432–47.
Gerea M. The importance of mixotrophic algae in the microbial food webs of shallow lakes [PhD Thesis] Argentina: University of Comahue; 2013.
Gorski PR, Armstrong DE, Hurley JP, Krabbenhoft DP. Influence of natural dissolved organic carbon on the bioavailability of mercury to a freshwater alga. Environ Pollut 2008;154:116–23.
Higueras P, Oyarzun R, Kotnik J, Esbrí JM, Martínez-Coronado A, Horvat M, et al. Compilation of field surveys on gaseous elemental mercury (GEM) from contrasting environmental settings in Europe, South America, South Africa and China: separating fads from facts. Environ Geochem Health 2013. http://dx.doi.org/10.1007/s10653-013-9591-2.
Karimi R, Chen CY, Pickhardt PC, Fisher NS, Folt CL. Stoichiometric controls of mercury dilution by growth. Proc Natl Acad Sci U S A 2007;104(18):1–6.
Le Faucheur S, Campbell GC, Fortin C, Slaveykova VI. Interactions between mercury and phytoplankton: speciation, bioavailability, and internal handling. Environ Toxicol Chem 2014;33:1211–24.
Luengen AC, Flegal AR. Role of phytoplankton in mercury cycling in the San Francisco Bay estuary. Limnol Oceanogr 2009;54(1):23–40.
Luengen AC, Fisher NS, Bergamaschi BA. Dissolved organic matter reduces algal accumulation of methylmercury. Environ Toxicol Chem 2012;31(8):1712–9.
Luoma SN, Rainbow PS. Metal contamination in aquatic environments: science and lateral management. Cambridge: Cambridge University Press; 2008.
Mason RP, Reinfelder JR, Morel FMM. Uptake, toxicity, and trophic transfer of mercury in a coastal diatom. Environ Sci Technol 1996;30(6):1835–45.
Mason RP, Laporte J-M, Andres S. Factors controlling the bioaccumulation of mercury, methylmercury, arsenic, selenium, and cadmium by freshwater invertebrates and fish. Arch Environ Contam Toxicol 2000;38:283–97.
McCauley E. The estimation of the abundance and biomass of zooplankton in samples. A manual on methods for the assessment of secondary productivity in fresh waters. Oxford, UK: Blackwell Scientific; 1984. p. 228–65.
Mitra KJ, Flynn JM, Burkholder T, Berge A, Calbet JA, Raven E, et al. The role of mixotrophic protists in the biological carbon pump. Biogeosciences 2014;11:995–1005.
Nriagu J, Becker C. Volcanic emissions of mercury to the atmosphere: global and regional inventories. Sci Total Environ 2003;304:3–12.
Nusch EA. Comparison of different methods for chlorophyll and phaeopigment determ. Arch Hydrobiol 1980;14:14–6.
Pickhardt PC, Fisher NS. Accumulation of inorganic and methylmercury by freshwater phytoplankton in two contrasting water bodies. Environ Sci Technol 2007;41(1):125–31.
Pickhardt PC, Folt CL, Chen CY, Klaue B, Blum JD. Algal blooms reduce the uptake of toxic methylmercury in freshwater food webs. Proc Natl Acad Sci U S A 2002;99(7):4419–23.
Pickhardt PC, Folt CL, Chen CY, Klaue B, Blum JD. Impacts of zooplankton composition and algal enrichment on the accumulation of mercury in an experimental freshwater food web. Sci Total Environ 2005;339:89–101.
Porter KG, Feig YS. The use of DAPI for identifying aquatic microflora. Limnol Oceanogr 1980;25:943–8.
Queimaliños C. The role of phytoplanktonic size fractions in the microbial food webs in two north Patagonian lakes (Argentina). Verh Int Ver Limnol 2002;28:1236–40.
Queimaliños CP, Modenutti BE, Balseiro EG. Phytoplankton responses to experimental enhancement of grazing pressure and nutrient recycling in a small Andean lake. Freshwat Biol 1998;40(1):41–9.
Queimaliños CP, Modenutti BE, Balseiro EG. Symbiotic association of the ciliate *Ophrydium naumanni* with *Chlorella* causing a deep chlorophyll a in an oligotrophic South Andean lake. J Plankton Res 1999;21:167–78.
Quirós R, Drago E. The environmental state of the Argentinean lakes: an overview. Lakes Reserv Res Manag 1999;4:55–64.
Rajamani S, Siripornadulsil S, Falcao V, Torres M, Colepicolo P, Sayre R. Phycorremediation of heavy metals using transgenic microalgae. In: León R, Galván Cejudo A, Fernández E, editors. Transgenic microalgae as green cell factories, 616. Book series: advances in experimental medicine and biology; 2007. p. 99–107.
Ravichandran M. Interactions between mercury and dissolved organic matter: a review. Chemosphere 2004;55:319–31.
Reinfelder JR, Fisher NS. The assimilation of elements ingested by marine copepods. Science 1991;251:794–6.
Ribeiro Guevara S, Žižek S, Repinc U, Pérez-Catán S, Jaćimović R, Horvat M. Novel methodology for the study of mercury methylation and reduction in sediments and water using ^{197}Hg radiotracer. Anal Bioanal Chem 2007;387:2185–97.
Ribeiro Guevara S, Meili M, Rizzo A, Daga R, Arribére MA. Sediment records of highly variable mercury inputs to mountain lakes in Patagonia during the past millennium. Atmos Chem Phys 2010;10:3443–53.
Rizzo A, Arcagni M, Campbell L, Koron N, Pavlin M, Arribére MA, et al. Source and trophic transfer of mercury in plankton from an ultraoligotrophic lacustrine system (Lake Nahuel Huapi, North Patagonia). Ecotoxicology 2014. http://dx.doi.org/10.1007/s10646-014-1260-4.
Stewart AR, Saiki MK, Kuwabara JS, Alpers CN, Marvin-DiPasquale M, Krabbenhoft DP. Influence of plankton mercury dynamics and trophic pathways on mercury concentrations of top predator fish of a mining-impacted reservoir. Can J Fish Aquat Sci 2008;65:2351–66.
Stoecker DK. Mixotrophy among dinoflagellates. J Eukaryot Microbiol 1999;46:397–401.
Sun J, Liu DY. Geometric models for calculating cell biovolume and surface area for phytoplankton. J Plankton Res 2003;25:1331–46.
Sunda WG, Huntsman SA. Processes regulating cellular metal accumulation and physiological effects: phytoplankton as model systems. Sci Total Environ 1998;219:165–81.
Twining BS, Fisher NS. Trophic transfer of trace metals from protozoa to mesozooplankton. Limnol Oceanogr 2004;49(1):28–39.
Twiss MR, Campbell PGC. Regeneration of trace metals from picoplankton by nanoflagellate grazing. Limnol Oceanogr 1995;40(8):1418–29.
Twiss MR, Campbell PGC. Trace metal cycling in the surface waters of Lake Erie: linking ecological and geochemical fates. J Great lakes Res 1998;24:791–807.
Twiss MR, Campbell PGC, Auclair JC. Regeneration, recycling, and trophic transfer of trace metals by microbial food-web organisms in the pelagic surface waters of Lake Erie. Limnol Oceanogr 1996;41(7):1425–37.
Twiss MR, Twining BS, Fisher NS. Partitioning of dissolved thallium by seston in Lakes Erie and Ontario. Can J Fish Aquat Sci 2003;60:1369–75.
Ullrich SM, Tanton TW, Abdrashitova SA. Mercury in the aquatic environment: a review of factors affecting methylation. Crit Rev Environ Sci Technol 2001;31(3):241–93.
Utermöhl H. Zur Vervollkommung der quantitativen Phytoplanktonmethodik. Mitt Int Ver Theor Angew Limnol 1958;9:1–38.
Wang Q, Kim D, Dionysiou DD, Sorial GA, Timberlake D. Sources and remediation for mercury contamination in aquatic systems — a literature review. Environ Pollut 2004;131:323–36.
Wu Y, Wang W-X. Intracellular speciation and transformation of inorganic mercury in marine phytoplankton. Aquat Toxicol 2014;148:122–9.
Zagarese HE, Diaz M, Pedrozo F, Ferraro M, Cravero W, Tartarotti B. Photodegradation of natural organic matter exposed to fluctuating levels of solar radiation. J Photochem Photobiol B 2001;61:35–45.